Incoherent Bragg reflection and Fermi-surface hot spots in a quasi-two-dimensional metal

I. Mihut,[1,2] C. C. Agosta,[1] C. Martin,[1] C. H. Mielke,[2] T. Coffey,[2] M. Tokumoto,[3] M. Kurmoo,[4] J. A. Schlueter,[5] P. Goddard,[2] and N. Harrison[2]

[1]*Department of Physics, Clark University, 950 Main Street, Worcester, Massachusetts 01610, USA*

[2]*National High Magnetic Field Laboratory, LANL, Los Alamos, New Mexico 87545, USA*

[3]*Nanotechnology Research Institute, AIST, Tsukuba 905-8568, Japan*

[4]*The Royal Institution, 21 Albemarle Street, London W1X 4BS, United Kingdom*

[5]*Materials Science Division, Argonne National Laboratory, Argonne, Illinois 60439, USA*

(Received 19 October 2005; revised manuscript received 13 December 2005; published 27 March 2006)

We propose a mechanism whereby a finite correlation length associated with the periodicity of the crystalline lattice gives rise to incoherent Bragg reflection of quasiparticles. This introduces an additional effective scattering rate $\tau_{\mathrm{hot}}^{-1}[\mathbf{k}_{\mathrm{F}}]$ that selectively damps quantum oscillations originating from orbits that are the product of Bragg reflection. The model is applied to the dimerization in κ-(BEDT-TTF)$_2$Cu(NCS)$_2$ where we show that $\tau_{\mathrm{hot}}^{-1}[\mathbf{k}_{\mathrm{F}}]$ is strongly dependent on the Fermi momentum $\mathbf{k}_{\mathrm{F}}$, being concentrated at "hot spots" located on the Brillouin zone boundary.

DOI: 10.1103/PhysRevB.73.125118 PACS number(s): 71.45.Lr, 71.18.+y, 71.20.Ps

Strongly anisotropic scattering processes have been proposed as an important factor in determining the unconventional physical properties of a variety of strongly correlated electron systems, including high-temperature superconductors,[1] organic conductors,[2,3] and heavy-fermion antiferromagnets.[4] In three-dimensional (3D) metals, magnetic quantum oscillation experiments can provide a means for probing such anisotropies directly. When a magnetic field **H** is applied in a given direction, only the extremal cyclotron orbits in momentum space orthogonal to **H** contribute significantly to the oscillation amplitude, enabling **H** orientation-dependent studies to selectively study different parts of the Fermi surface. Since the effective mass $m^*[\mathbf{k}_{\mathrm{F}}]$ and quasiparticle scattering rate $\tau^{-1}[\mathbf{k}_{\mathrm{F}}]$ vary over the Fermi surface, quantum oscillation experiments can enable their orbital averages $(m^* = eB/2\pi \oint \mathrm{d}t \propto \oint m^*[\mathbf{k}_{\mathrm{F}}]\mathrm{d}k_{\parallel}$ and $\tau^{-1} = eB/2\pi m^* \oint \tau^{-1}[\mathbf{k}_{\mathrm{F}}]\mathrm{d}t)$ to be determined as a function of the orientation of **H**, where $B \approx \mu_0|\mathbf{H}|$ and $\mathbf{k}_{\mathrm{F}}$ is the Fermi momentum.

Such studies have been successfully applied to cubic materials with near-spherical Fermi surfaces, enabling detailed maps of $m^*[\mathbf{k}_{\mathrm{F}}]$ and $\tau^{-1}[\mathbf{k}_{\mathrm{F}}]$ to be extracted.[4–6] However, many of the more strongly correlated superconductors of interest today have layered electronic structures[1,2,7,8] yielding Fermi surfaces that are highly 2D. While "hot spots" in which correlations are enhanced due to spin fluctuations have been predicted in both high-temperature superconductors[1] and organic conductors,[3] their 2D geometry prohibits a direct observation. The absence of closed extremal orbits when **H** is oriented within the layers implies that **H** orientation-dependent quantum oscillation studies cannot be used to extract information on the anisotropy of $m^*[\mathbf{k}_{\mathrm{F}}]$ and $\tau^{-1}[\mathbf{k}_{\mathrm{F}}]$ within the layers. The finding of an alternative means to verify (or falsify) the existence of hot spots could have a decisive impact on attempts to identify the appropriate theories for superconductivity.

In this paper we propose that magnetic breakdown (MB), in which the magnetic field facilitates the tunneling of quasiparticles through band gaps, may provide an alternative means for probing the existence of hot spots. We consider the analogous case of incoherent Bragg reflection (IBR), which can cause $\tau^{-1}[\mathbf{k}_{\mathrm{F}}]$ to be strongly concentrated at the Brillouin zone boundary as depicted in Fig. 1. κ-(BEDT-TTF)$_2$Cu(NCS)$_2$ has the ideal Fermi surface topology[7] to test the possibility of phase decoherence of quasiparticles undergoing Bragg reflection in a weakly disordered crystalline lattice. IBR selectively dephases quasiparticles on the α orbit in Fig. 1 undergoing Bragg reflection as opposed to those for which MB facilitates tunneling across the band gap $2\Delta_{\mathrm{g}}$. MB enables quasiparticles on the MB β orbit to follow the dotted lines near the Brillouin zone boundary in Fig. 1, causing them to be no longer affected by Bragg reflection. To explain the experimentally observed

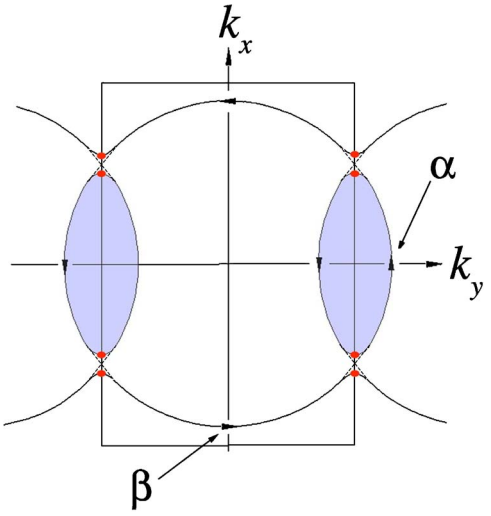

FIG. 1. (Color online) A schematic of the Fermi surface of κ-(BEDT-TTF)$_2$Cu(NCS)$_2$ before (dotted lines) and after (solid lines) its reconstruction due to Bragg reflection at the Brillouin zone boundary. The red dots indicate the proposed positions of hot spots at the Brillouin zone boundary.

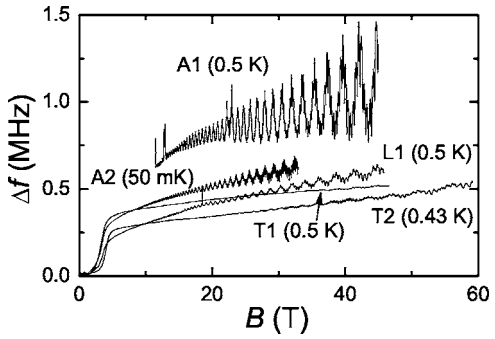

FIG. 2. Examples of the shift in the TDO frequency due to the sample's finite resistivity, displayed for five different samples T1 and T2, grown in Tsukuba, A1 and A2 grown in Argonne and L1 grown in London.

large ratio $\tau_\alpha^{-1}/\tau_\beta^{-1}$ of the total orbitally averaged effective scattering rates for the two orbits, we develop a model for an "effective" scattering rate $\tau_{\text{hot}}^{-1}[\mathbf{k}_F]$ due to IBR.

The experiments are conducted on five single crystals of κ-(BEDT-TTF)$_2$Cu(NCS)$_2$ obtained from three different crystal growth facilities, each crystal being of comparable volume (0.1 mm^3).[9] When placed in the coil of a tunnel diode oscillator (TDO) circuit, the crystal's finite in-plane resistivity causes a perturbation of its inductance, leading to a shift Δf in resonance frequency.[10] Figure 2 shows raw data obtained for *all* five samples in pulsed and static magnetic fields. To ensure that estimates of m^* and τ^{-1} are independent of the measurement technique, comparisons are made with data obtained using conventional four-wire resistance methods. In all cases, the respective quantum oscillation frequencies $F_\alpha \approx 600$ T and $F_\beta \approx 3900$ T and effective masses $m_\alpha^* \approx 3.5 m_e$ and $m_\beta^* \approx 7.0 m_e$ for the α and β orbits are found to be the same to within experimental uncertainty, confirming that all samples are of the *same* κ-(BEDT-TTF)$_2$Cu(NCS)$_2$ phase.

Figure 3 compares "Dingle plots"[19] for the α and β orbits in which the oscillatory component of the in-plane resistivity (determined by Fourier analysis) is renormalized by the average background (nonoscillatory) magnetoresistance[20] and then subsequently divided by the thermal damping factor $R(T)=X/\sinh X$ (where $X=2\pi^2 m^* k_B T/\hbar e B$, inserting values for m_α^* and m_β^*). The logarithm of the remaining amplitudes have field dependences[11–17]

$$\ln A_\alpha(B) = C_\alpha + \eta \ln B - \pi m_\alpha^* \tau_\alpha^{-1}/eB + \ln[1 - e^{-B_0/B}],$$

$$\ln A_\beta(B) = C_\beta + \eta \ln B - (\pi m_\beta^* \tau_\beta^{-1}/e + 2B_0)/B, \qquad (1)$$

where $\eta=0$ for Shubnikov–de Haas oscillations in a near ideal 2D layered metal[14] and C_α and C_β are constants. $B_0 = \pi m_\beta^* \Delta_g^2/\hbar e E_F \sin 2\theta$ is the characteristic MB field,[19] where $2\Delta_g$ is the band gap due to dimerization (which should be sample independent), $E_F=\hbar e F_\beta/m_\beta^*$ is the Fermi energy, and 2θ is the angle of Bragg reflection. Fits of Eq. (1) to such Dingle plots yield B_0, τ_α^{-1}, and τ_β^{-1}.

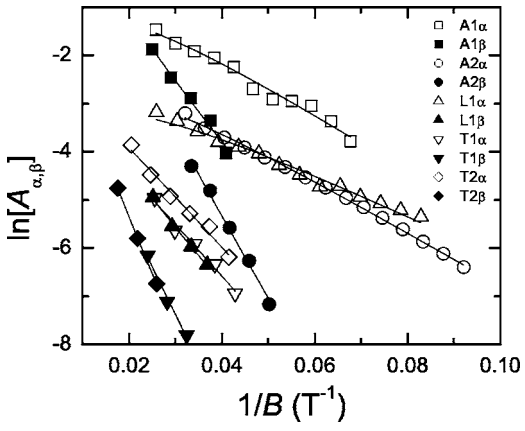

FIG. 3. Dingle plots of $\ln A_\alpha$ and $\ln A_\beta$ versus $1/B$ having corrected for $R(T)$ and renormalized the amplitude of the quantum oscillations by the background magnetoresistance, together with fits to Eq. (1) shown for $B_0=38$ T (see text).

While there exists a broad consensus regarding m_α^* and m_β^*, estimates of B_0 vary considerably throughout the literature,[11–17] yielding $B_0=40\pm6$ T when including all prior estimates obtained using $\eta=0$ as for a 2D metal. The large error reveals the difficulty associated with obtaining a convergence in B_0 far from the ideal MB experimental condition $B \gg B_0$. We encounter a similar lack of convergence on fitting Eq. (1) to the α-frequency Dingle plots in Fig. 3, yielding $B_0=45\pm22$ T, 38 ± 8 T, and 45 ± 59 T for samples A1, A2, and L1, respectively, or a culminated value of 39 ± 7 T. In the case of samples T1 and T2, fits do not converge owing to the relatively short range in magnetic field over which oscillations are observed. To make allowance for the large error bars in B_0, we therefore plot τ_α^{-1} and τ_β^{-1} for a wide range of B_0 ($0<B_0<60$ T) in Fig. 4(a).

Information on the anisotropy of $\tau(\mathbf{k}_F)$ can be extracted because the quasiparticles on the α and β orbits traverse different trajectories in k space in Fig. 1. This enables us to resolve different average rates τ_1^{-1} and τ_2^{-1} for quasiparticles on the quasi-1D and quasi-2D Fermi surface sections, respectively. If we choose to neglect the gap by setting $\Delta_g \to 0$, consideration of the proportionate times $t_1=2\pi(m_\beta^* - m_\alpha^*)/eB$ and $t_2=2\pi m_\alpha^*/eB \approx t_1$ spent by the quasiparticles on each section yields $\tau_\alpha^{-1}=\tau_2^{-1}$ and $\tau_\beta^{-1}=(t_1\tau_1^{-1}+t_2\tau_2^{-1})/(t_1+t_2) \approx (\tau_1^{-1}+\tau_2^{-1})/2$. Hence

$$\frac{\tau_\alpha^{-1}}{\tau_\beta^{-1}} = \frac{2\tau_2^{-1}}{\tau_1^{-1}+\tau_2^{-1}} \leqslant 2. \qquad (2)$$

It is quite clear that no degree of anisotropy of $\tau(\mathbf{k}_F)$ can explain values of the ratio $\tau_\alpha^{-1}/\tau_\beta^{-1}$ in Fig. 4(b) that exceed 2. If we attempt to extract τ_2^{-1}/τ_1^{-1} [dashed line in Fig. 4(b)] from the five-sample averaged $\tau_\alpha^{-1}/\tau_\beta^{-1}$ (solid line), we find that τ_2^{-1}/τ_1^{-1} becomes asymptotic for $B_0 \approx 30$ T: i.e., there is no viable τ_2^{-1}/τ_1^{-1} solution for any of the fitted estimates of B_0 that assume a 2D Fermi surface.[13–17]

If $B_0>30$ T, as the fits suggest, only by considering a finite Δ_g can we explain $\tau_\alpha^{-1}/\tau_\beta^{-1}>2$. The opening of such a gap enables quasiparticles on the α and β orbits to take slightly different paths in the vicinity of the Brillouin zone boundary in Fig. 1. A strong enhancement of $\tau(\mathbf{k}_F)$ at the points represented by red spots in Fig. 1 can only contribute

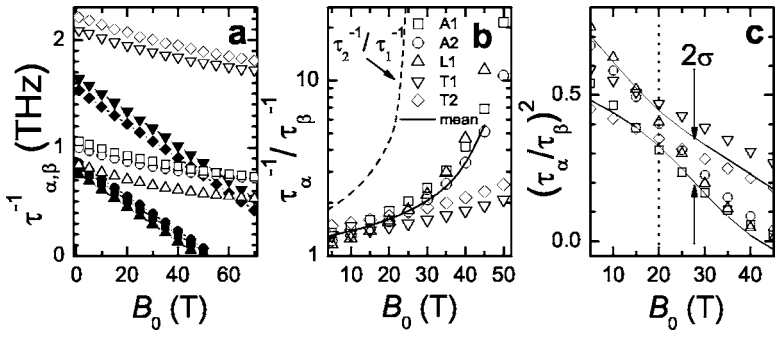

FIG. 4. (a) Scattering rates determined from Fig. 3 as a function of B_0. (b) The ratio $\tau_\alpha^{-1}/\tau_\beta^{-1}$ as a function of B_0. The dashed line represents τ_2^{-1}/τ_1^{-1} estimated using Eq. (2). (c) Plot of $(\tau_\alpha/\tau_\beta)^2$ with the solid lines representing $(\tau_\alpha/\tau_\beta)^2 \pm \sigma$ to estimate the value of B_0 (dotted line) where convergence occurs.

to τ_α^{-1} because only these quasiparticles are modified by Bragg reflection. On introducing an additional hot spot scattering rate $\tau_{\rm hot}^{-1}$ that contributes only to the orbitally averaged scattering time of the α orbit, we can revise Eq. (2) so that it becomes

$$\frac{\tau_\alpha^{-1}}{\tau_\beta^{-1}} \approx \frac{2(\tau_2^{-1}+\tau_{\rm hot}^{-1})}{\tau_1^{-1}+\tau_2^{-1}}, \tag{3}$$

which can now assume any value.[18]

We propose IBR as the mechanism that can lead to the additional $\tau_{\rm hot}^{-1}(\mathbf{k}_{\rm F})$ in the vicinity of the Brillouin zone boundary. The standard theory of Bragg reflection assumes the crystalline potential responsible for the gap to remain periodic over all space.[19] In real materials, however, the lattice is subject to imperfections due to dislocations, cracks, and voids that cause the periodicities over long distances to become uncorrelated. This leads to a loss of coherence of the Bloch waves over similar distances, leading to finite mean free paths λ and scattering times τ in accordance with the standard semiclassical description. In addition to being subjected to conventional pointlike scattering processes, quasiparticles with large momentum vectors that suffer diffraction from the lattice will also be subjected to an uncertainty in their momentum of order $\Delta\hbar k = \hbar/2\xi$ upon undergoing Bragg reflection, where ξ represents the finite correlation length of the lattice periodicity of interest. In the case of κ-(BEDT-TTF)$_2$Cu(NCS)$_2$, it is the dimerization along the c axis that causes Bragg reflection. Its characteristic vector $\mathbf{K} = [0, 2\pi/c, 0]$ intersects the large free-electron-like β hole orbit, leading to the opening of $2\Delta_{\rm g}$ and the formation of the α orbit in Fig. 1.

One can conveniently treat the dephasing of quasiparticles in a semiclassical picture by considering an imaginary contribution to the Onsager phase and/or k-space area. In the case of IBR, $\Delta\hbar k$ introduces an imaginary contribution

$$\mathrm{Im}[a_\alpha] = \frac{ik_\alpha}{\xi} \tag{4}$$

to the cross-sectional area of the α orbit in k space, such that $a_\alpha = \mathrm{Re}[a_\alpha] + \mathrm{Im}[a_\alpha]$, where $i = \sqrt{-1}$ and $\mathrm{Re}[a_\alpha]$ is its usual area (i.e., as in the limit $\xi^{-1} \to 0$) which has roughly the shape of a lens with a major axis length $2k_\alpha \approx 0.52\ 2\pi/b \approx 1/2.6\ \text{Å}^{-1}$.[17] The imaginary contribution to the Onsager phase Φ_α due to IBR becomes

$$\frac{\partial\,\mathrm{Im}[\Phi_\alpha]}{\partial t} = \left(\frac{\hbar}{eB}\right)\frac{\partial\,\mathrm{Im}[a_\alpha]}{\partial t} \equiv \frac{i}{2\tau_{\rm hot}[\mathbf{k}_{\rm F}]}, \tag{5}$$

enabling us to introduce an effective scattering rate $\tau_{\rm hot}^{-1}(\mathbf{k}_{\rm F})$. On calculating its orbital average, we obtain

$$\tau_{\rm hot}^{-1} = \frac{eB}{2\pi m_\alpha^*}\oint \frac{\mathrm{d}t}{\tau_{\rm hot}[\mathbf{k}_{\rm F}]} = \frac{\hbar k_\alpha}{\pi\xi m_\alpha^*}. \tag{6}$$

Should $\tau_1^{-1} \approx \tau_2^{-1}$ in Eq. (3), then $B_0 \approx 39$ T yields $\tau_{\rm hot}^{-1} \approx \tau_\alpha^{-1} - \tau_\beta^{-1} \approx 0.5 \times 10^{12}\ \text{s}^{-1}$ for the best samples, corresponding to $2\xi \approx 3000\ \text{Å} \sim 180c$, which is of comparable magnitude to the mean free path $\lambda = \hbar k_\beta \tau_\beta / m_\beta^* \sim 2000$ Å for normal collision processes that account for most of attenuation of the quantum oscillations originating from the β orbit, suggesting that λ and ξ probably originate from common defects in the lattice.

In order to show that $\tau_{\rm hot}^{-1}$ is concentrated at hot spots, it is necessary to calculate the full dependence of $\tau_{\rm hot}^{-1}(\mathbf{k}_{\rm F})$ on $\mathbf{k}_{\rm F}$. According to the Fermi-surface model in Fig. 1, the free electron-like hole quasiparticle orbits intersect each other approximately at right angles upon their translation by $\mathbf{K}$. It is therefore convenient to model the local dispersion in the vicinity of the Brillouin zone boundary by two orthogonal bands of the form

$$\varepsilon[\mathbf{k}] = \frac{\hbar v_\beta}{\sqrt{2}}\left[k_x \pm \left(k_y + \frac{i}{4\xi}\right)\right], \tag{7}$$

represented by dotted lines in Fig. 5(a) (for the limit $\xi^{-1} \to 0$). Here, they are defined with respect to $k_x = 0$ and $k_y = 0$ at the point of intersection, where $i/2\xi$ is the difference in

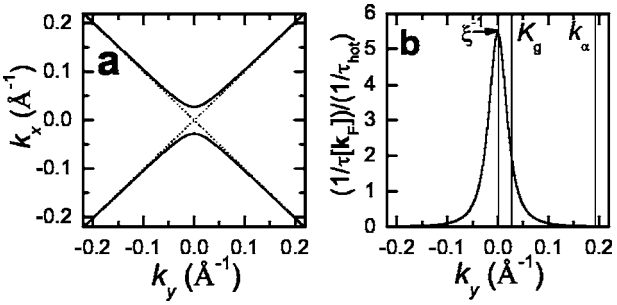

FIG. 5. (a) A plot of the Fermi surface topology in the vicinity of the Brillouin zone boundary as a consequence of Bragg reflection. (b) A plot of the calculated ratio $\tau_{\rm hot}^{-1}[\mathbf{k}_{\rm F}]/\tau_{\rm hot}^{-1}$ according to the model as a function of the momentum vector k_y parallel to $\mathbf{K}$.

k_y between them due to the effect of a finite correlation length. Hybridization yields

$$\varepsilon[\mathbf{k}] = \frac{\hbar v_\beta}{\sqrt{2}}\left[k_x \pm \sqrt{\left(k_y + \frac{i}{4\xi}\right)^2 + K_g^2}\right], \tag{8}$$

where $K_g^{-1} = \hbar v_\beta / \sqrt{2}\Delta_g \approx 35$ Å for $B_0 \approx 39$ T. The hybridized bands are represented by solid lines in Fig. 5(a) (again, for the limit $\xi^{-1} \to 0$). Action of the Lorentz force $\hbar \partial \mathbf{k}/\partial t = e\mathbf{v}_F \times \mathbf{B}$ on quasiparticles moving at a velocity $\mathbf{v}_F[\mathbf{k}] = \hbar^{-1}\nabla_{\mathbf{k}}\varepsilon[\mathbf{k}]$ in a magnetic field yields

$$\mathbf{k}_F[t] \approx \left\{ \pm \sqrt{\left[\left(\frac{eBv_\beta}{\sqrt{2}\hbar}\right)t + \frac{i}{4\xi}\right]^2 + K_g^2}, \left(\frac{eBv_\beta}{\sqrt{2}\hbar}\right)t, 0 \right\}. \tag{9}$$

The time evolution of the k-space area is approximately given by $\partial \mathrm{Im}[a_\alpha]/\partial t \approx \partial |\mathbf{k}_F \times \mathrm{Im}[\mathbf{k}_F]|/\partial t$ where $\mathbf{k}_F \approx [k_\beta/\sqrt{2}, k_\beta/\sqrt{2}, 0]$ is the Fermi momentum vector and $k_\beta \approx \sqrt{2}k_\alpha$. On evaluating $\mathrm{Im}[\mathbf{k}_F]$ from Eq. (9) in the limit $(eBv_\beta/\sqrt{2}\hbar)t \ll 4\xi K_g^2$, insertion of $\partial \mathrm{Im}[a_\alpha]/\partial t$ into Eq. (5) yields, after some manipulation,

$$\frac{1}{\tau_{hot}[\mathbf{k}_F]} \approx \frac{\pi}{4}\frac{k_\alpha(K_g^2 - 1/16\xi^2)}{(k_y^2 + K_g^2 - 1/16\xi^2)^{3/2}}\frac{1}{\tau_{hot}}. \tag{10}$$

Figure 5(b) shows the dependence of $\tau_{hot}^{-1}[\mathbf{k}_F]$ on k_y according to Eq. (10), revealing that ≈70 and 90% of the scattering intensity occur within $|k_y| < K_g$ and $|k_y| < 2K_g$, respectively. This shows quite clearly that the bulk of the "attenuation" occurs close to the Brillouin zone boundary.

In summary, we propose a mechanism whereby a finite correlation length ξ of the weakly disordered crystalline lattice in κ-(BEDT-TTF)$_2$Cu(NCS)$_2$ causes incoherent Bragg reflection of quasiparticles at the Brillouin zone boundary. This introduces an additional effective scattering rate $\tau_{hot}^{-1}[\mathbf{k}_F]$ that selectively damps quantum oscillations originating from the α orbits in κ-(BEDT-TTF)$_2$Cu(NCS)$_2$. This can cause the ratio of the orbitally averaged scattering rates $\tau_\alpha^{-1}/\tau_\beta^{-1}$ to exceed 2. Model calculations show that $\tau_{hot}^{-1}[\mathbf{k}_F]$ is strongly dependent on the Fermi momentum $\mathbf{k}_F$, being concentrated at hot spots located on the Brillouin zone boundary. IBR may therefore explain a number of unusual experimental results in disordered κ-phase salts in which oscillations from the β MB orbit are clearly observed in quantum oscillation experiments, but where those from the α orbit are vanishingly small or absent.[21,22]

This work is supported by the U.S. Department of Energy, the National Science Foundation, and the State of Florida. We would like to thank Steve Blundell and John Singleton for inspiring a revision of the model description.

[1] R. Hlubina and T. M. Rice, Phys. Rev. B **51**, 9253 (1995).
[2] P. M. Chaikin, Phys. Rev. Lett. **69**, 2831 (1992).
[3] J. Schmalian, Phys. Rev. Lett. **81**, 4232 (1998).
[4] T. Ebihara, N. Harrison, M. Jaime, S. Uji, and J. C. Lashley, Phys. Rev. Lett. **93**, 246401 (2004).
[5] M. Springford, Adv. Phys. **20**, 493 (1971); D. H. Lowndes *et al.*, Proc. R. Soc. London, Ser. A **331**, 497 (1973).
[6] D. McK Paul and M. Springford, J. Phys. F: Met. Phys. **8**, 1713 (1978).
[7] J. Singleton, Rep. Prog. Phys. **63**, 1111 (2000).
[8] R. Settai, H. Shishido, S. Ikeda, Y. Murakawa, D. Aoki, Y. Haga, H. Harima, and Y. Onuki, J. Phys.: Condens. Matter **13**, L627 (2001).
[9] I. Mihut *et al.* (unpublished).
[10] T. Coffey, Z. Bayindir, J. F. DeCarolis, M. Bennet, G. Esper, and C. C. Agosta, Rev. Sci. Instrum. **71**, 4600 (2000).
[11] T. Sasaki, H. Sato, and N. Toyota, Physica C **185–189**, 2687 (1991).
[12] J. Caulfield, W. Lubczynski, F. L. Pratt, J. Singleton, D. Y. K. Ko, W. Hayes, M. Kurmo, and P. Day, J. Phys.: Condens. Matter **6**, 2911 (1994).
[13] F. A. Meyer, E. Steep, W. Biberacher, P. Christ, A. Lerf, A. G. M. Jansen, W. Joss, P. Wyder, and K. Andres, Europhys. Lett. **32**, 681 (1995).
[14] N. Harrison, J. Caulfield, J. Singleton, P. H. P. Reinders, F. Herlach, W. Hayes, M. Kurmoo, and P. Day, J. Phys.: Condens. Matter **8**, 5415 (1996).
[15] S. Uji, M. Chaparala, S. Hill, P. S. Sandhu, J. Qualls, L. Seger, and J. S. Brooks, Synth. Met. **85**, 1573 (1997).
[16] T. Biggs, A. K. Klehe, J. Singleton, D. Bakker, J. Symington, P. Goddard, A. Ardavan, W. Hayes, J. A. Schlueter, T. Sasaki, and M. Kurmoo, J. Phys.: Condens. Matter **14**, L495 (2002).
[17] P. A. Goddard, S. J. Blundell, J. Singleton, R. D. McDonald, A. Ardavan, A. Narduzzo, J. A. Schleuter, A. M. Kini, and T. Sasaki, Phys. Rev. B **69**, 174509 (2004).
[18] Given the large experimental uncertainty in B_0 estimates, the convergence of $(\tau_\alpha/\tau_\beta)^2$ at $B_0 \sim 20$ T in Fig. 4(c) (inverted and squared simply to obtain a linear plot) may provide an alternative estimate of $B_0 = 20 \pm 5$ T. The validity of this alternative analysis nevertheless requires the scattering contributions to $\tau_{1,2}^{-1}$ and τ_{hot}^{-1} to be proportionately affected by the same crystalline defects. This would require an independent microstructural analysis to determine whether or not a single type of defect dominates.
[19] D. Shoenberg, *Magnetic Oscillations in Metals* (Cambridge University Press, Cambridge, England, 1984).
[20] The prefactor for the in-plane oscillatory component of the magnetoresistance of a 2D metal is approximately independent of H: P. T. Coleridge, Phys. Rev. B **44**, 3793 (1991).
[21] C. H. Mielke, N. Harrison, D. G. Rickel, A. H. Lacerda, R. M. Vestal, and L. K. Montgomery, Phys. Rev. B **56**, R4309 (1997).
[22] N. Harrison, C. H. Mielke, D. G. Rickel, L. K. Montgomery, and T. Burgin, Phys. Rev. B **56**, R12905 (1997).